Conformational Transitions in RNA Single Uridine and Adenosine Bulge Structures: A Molecular Dynamics Free Energy Simulation Study

André Barthel and Martin Zacharias
School of Engineering and Science, International University Bremen, D-28759 Bremen, Germany

ABSTRACT Extra unmatched nucleotides (single base bulges) are common structural motifs in folded RNA molecules and can participate in RNA-ligand binding and RNA tertiary structure formation. Often these processes are associated with conformational transitions in the bulge region such as flipping out of the bulge base from an intrahelical stacked toward a looped out state. Knowledge of the flexibility of bulge structures and energetics of conformational transitions is an important prerequisite to better understand the function of this RNA motif. Molecular dynamics simulations were performed on single uridine and adenosine bulge nucleotides at the center of eight basepair RNA molecules and indicated larger flexibility of the bulge bases compared to basepaired regions. The umbrella sampling method was applied to study the bulge base looping out process and accompanying conformational and free energy changes. Looping out toward the major groove resulted in partial disruption of adjacent basepairs and was found to be less favorable compared to looping out toward the minor groove. For both uridine and adenosine bulges, a positive free energy change for full looping out was obtained which was $\sim$1.5 kcal mol^{-1} higher in the case of the adenosine compared to the uridine bulge system. The simulations also indicated stable partially looped out states with the bulge bases located in the RNA minor groove and forming base triples with 5′-neighboring basepairs. In the case of the uridine bulge this state was more stable than the intrahelical stacked bulge structure. Induced looping out toward the minor groove involved crossing of an energy barrier of $\sim$3.5 kcal mol^{-1} before reaching the base triple state. A continuum solvent analysis of intermediate bulge states indicated that electrostatic interactions stabilize looped out and base triple states, whereas van der Waals interactions and nonpolar contributions favor the stacked bulge conformation.

INTRODUCTION

Besides double stranded regions, folded RNA molecules frequently contain mismatches, internal loops, hairpin loops, and extra unpaired bases (bulges). These secondary structure motifs can be of functional importance for ligand binding, catalysis, and protein recognition during regulation of gene expression (1–7). Extra bases that lack a pairing partner in the complementary strand, known as bulges, are one of the most abundant motifs in many biological RNA molecules (6,8,9). A structural property of regular double stranded A-form RNA is the deep and narrow major groove, which is hardly accessible to ligands or peptides for complex formation. Additional extra bulge bases can introduce bends and kinks into RNA helices that result in a partial unwinding of the helix and an opening of the major groove (10–14). Bulges in double stranded RNA do not only affect ligand binding indirectly by changing the helical structure but may also participate directly in specific binding interactions (15–17). For example, the transactivation response element (TAR) of the human immunodeficiency virus contains a three-nucleotide bulge structure that is recognized by the viral Tat protein and undergoes conformational changes from a partially stacked to a looped out form that involves formation of a base triple upon Tat binding (18–21). The *Escherichia coli* MS2 phage coat protein binding site (22) is an RNA hairpin tetraloop containing a single adenosine bulge. In the unbound state the adenine bulge base stacks into the helical RNA stem (23). The bulge conformation changes to an extrahelical looped out state upon binding of the viral coat protein (15).

Structural studies, e.g., x-ray crystallography or NMR spectroscopy can give insights into the importance of single and multiple bulges in RNA for specific interactions with proteins, peptides, and other ligands. However, structural analysis alone gives only little information on the structural flexibility of bulge elements and the energetics of structural transitions in this motif. Knowledge of the free energy contribution of structural transitions in bulge motifs such as the looping out of the bulge base upon ligand binding is important for the understanding of the mechanism of induced fit binding to RNA.

Molecular dynamics (MD) simulations can be helpful to elucidate the mechanism of the bulge base looping out process and to give an estimate of the associated change in free energy. The MD approach has been used extensively to study nucleic acids (24) including studies of bulge-containing RNA and DNA (25,26). It is also possible to enforce structural transitions in MD simulations by adding a penalty potential (umbrella potential) that biases the sampled conformations toward a desired state. Such umbrella sampling calculations allow us to extract the work or free energy required to achieve a structural transition in the target molecule. For example DNA repair and methylation requires the coupled breaking of a basepair (bp) and flipping out of one

Submitted October 17, 2005, and accepted for publication December 6, 2005.

Address reprint requests to Martin Zacharias, School of Engineering and Science, International University Bremen, Campus Ring 1, D-28759 Bremen, Germany. Tel.: 49-421-200-3541; Fax: 49-421-200-3249; E-mail: m.zacharias@iu-bremen.de.

0006-3495/06/04/2450/13 $2.00

doi: 10.1529/biophysj.105.076158

base to interact with the repair or methylation enzyme (27). The umbrella sampling technique has been used to investigate the breaking of a bp and looping out of one base in several MD studies, resulting in associated free energy changes of ~10–23 kcal mol^{-1} (28–35). The looping out of an extra stacked bulge base in the absence of a complementary base in the second strand has so far not been studied. It is expected that this conformational change requires less free energy since no canonical Watson-Crick (WC) bp needs to be disrupted. In this study, looping out of single base bulges in A-form RNA has been studied using MD simulations and the umbrella sampling method. Since the presence of a bulge can destabilize a dsRNA molecule, an RNA model system consisting of eight G:C bps with a repeating CpG sequence and an extra bulge nucleotide between the fourth and the fifth bp was chosen. The single bulge is the simplest bulge motif allowing a systematic check of the convergence of the umbrella sampling calculations. Simulations were performed on uracil and adenine bulge bases representing pyrimidine and purine nucleo-bases, respectively. In addition to the looping out free energy profile, identification of intermediate structures associated with local minima in the free energy pathway has been possible. The parent canonical RNA (without the bulge nucleotide) was also investigated as a reference system to study the impact of the bulge conformation on the helical structure.

MATERIALS AND METHODS

All MD simulations were carried out with the AMBER 6 program suite and the parm94 force field (36). RNA bulge start structures (5′-CGCGBCGCG/5′-CGCGCGCG; with B being either adenosine or uridine) adopting a stacked bulge conformation were generated using the *nucgen* module of AMBER 6. Added to fill a cubic box were ~4000 TIP3P water molecules, leaving at least 10 Å between solute atoms and the boundaries of the box. Electroneutrality was achieved by adding 15 sodium counterions. Initial energy minimization (2000 steps) of the system was performed with the SANDER module of the AMBER 6 package. After minimization the systems were gradually heated up to 300 K with positional restraints (force constant 50 kcal mol^{-1} Å^{-2}) on RNA atoms over a period of 0.25 ns, allowing water molecules and ions to move freely. During an additional 0.25 ns, the positional restraints were gradually reduced to finally allow unrestrained MD simulation of all atoms over a subsequent total simulation time of 4 ns. The final structure of the equilibration run was used as the initial structure for the bulge base looping out. The long range electrostatic interactions were treated with the particle-mesh Ewald (PME) method using a cutoff distance of $r_{\text{cuttoff}} = 9$ Å. The SHAKE algorithm (37,38) was used to constrain bond vibrations involving hydrogen atoms, which allows a time step of $\tau = 2$ fs. Thermal equilibrium was achieved with the Berendsen thermostat (39). Helicoidal parameters of recorded structures were determined using the CURVES program (40,41). For comparison an 8 bp dsRNA without a bulge (5′-CGCGCGCG)$_2$ was equilibrated and analyzed in the same way as the bulge structures.

The umbrella sampling method was used to calculate the difference in free energy between the bulge RNA molecules in stacked and loop out conformations, respectively. The dihedral angle θ spanned by the atoms RB5.N1(N9), RB5.C1′, RC6.C1′, and RG13.C1′, where B denotes the bulge nucleotide, was chosen as the reaction coordinate (Fig. 1 *B*).

Umbrella potentials with a force constant $k = 0.06$ kcal mol^{-1} deg^{-2} ($k = 200$ kcal mol^{-1} rad^{-2}) were distributed uniformly along the reaction coordinates at a distance of $\Delta\theta_{\text{ref}} = 5°$. Consecutive sampling windows of θ were started from equilibrated structures of the last run in the previous set. The resulting calculated PMF depends on the timescale of the sampling runs and converged with increasing simulation time per sampling window. For the final potential of mean force (PMF) calculations, the systems were simulated for 2 ns per umbrella sampling window to achieve good convergence. The value of the dihedral angle θ was recorded every 0.1 ps. The potential of mean force was calculated from the recorded data sets using the WHAM (weighted histogram analysis method; 42–44) as implemented by Grossfield (45).

The MM-GBSA (molecular mechanics generalized-Born continuum solvent) approach (46–48) was applied to the RNA bulge sites for the umbrella sampling windows in the range $-35° \leq \theta \leq 145°$ to analyze energetic contributions to the bulge base looping out process. The bulge nucleotides as well as the flanking bps were extracted from the recorded trajectories of the umbrella sampling. The structures were evaluated using the generalized Born continuum model (49–51) as implemented in AMBER (36) using the mbondi set of atom radii (52) and a salt concentration of 0.15 mol l^{-1} in combination with a surface area dependent nonpolar solvation term. The total energy of a conformer (E_{pot}) is given as a sum of Coulomb (E_{Coul}), Lennard-Jones (E_{vdW}), bonded contributions, electrostatic solvation (E_{GB}), and nonpolar solvation contributions (E_{surf} characterized by a surface area tension coefficient, $\gamma = 0.005$ kcal mol^{-1} Å^{-2}).

RESULTS

Unrestrained molecular dynamics simulation of the RNA with intrahelical stacked bulge bases

Unrestrained MD simulations (4 ns) of the RNA molecules with intrahelical stacked bulge bases (Fig. 1 *A*) and of the 8

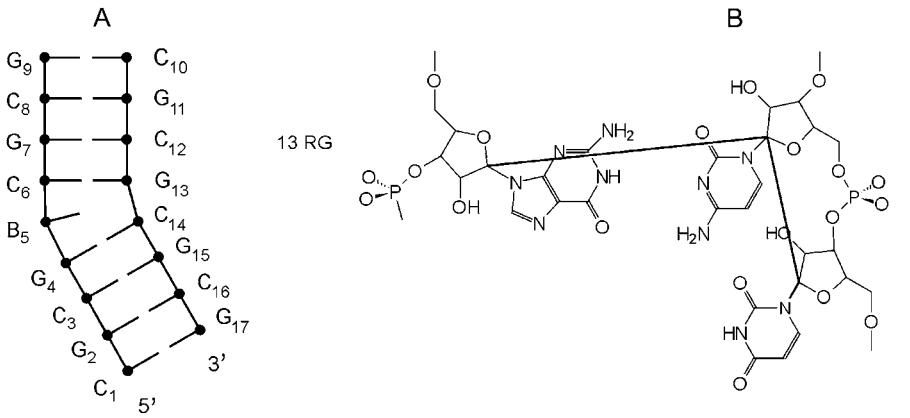

FIGURE 1 (*A*) Basepairing scheme of the single base bulge RNAs, B, denotes bulge nucleotides A or U. (*B*) Definition of the dihedral angle reaction coordinate θ used for umbrella sampling (indicated as *bold line* between N1 and C1′ atoms of the bulge base (5RU) and the C1′ atoms of the neighboring nucleotides 6 and 13).

bp dsRNA reference structure resulted in stable root mean square deviations (Rmsd) of the central parts of the molecules with respect to the start structures (data not shown). For the dsRNA reference structure, this agrees with an NMR study that indicates a fully paired structure for this sequence in solution (53). In the case of the uridine bulge some transient fraying (opening) of the terminal bp was observed. The dihedral angle θ as defined in Fig. 1 *B* was measured during the unrestrained simulations. This dihedral angle approximately describes the angular orientation of the bulge base with respect to the neighboring bp. In the case of the single uridine bulge, the dihedral angle is asymmetrically distributed over a wide range of angles from $-80°$ to $-20°$ with the maximum at $-57°$ (Fig. 2). A more positive value of θ indicates motion of the base toward the minor groove (a more negative value indicates looping toward the major groove of the RNA). The probability distribution P(θ) shows a longer tail toward lower absolute values of θ (minor groove conformations). In contrast, the P(θ) distribution of the adenosine bulge system (Fig. 2) is more symmetric, i.e., a bell shaped curve centered at $-40°$, and the distribution covers a range of $\sim 30°$, i.e., it is narrower than the distribution found for the uridine bulge system. Thus, the unrestrained simulations indicate a greater mobility of the stacked uracil bulge base than the adenine bulge base. A shoulder in the A bulge P(θ) appears that may arise from the occupation of an additional substate of the bulge.

To study possible base-base interactions involving the bulge base during unrestrained MD, the hydrogen bonding pattern between the bulge base and bases complementary to the bulge flanking bases was investigated (Fig. 3). The correlation plots reveal hydrogen bonding interactions between the bulge base and adjacent bps. In the case of the uridine bulge, in most of the trajectory snapshots the bulge flanking bps are intact and the uracil base does not interfere with the neighboring bp geometry. In a few snapshots the classical basepairing of the 5′ bulge flanking bp breaks and a noncanonical U·C bp is established. The lifetime of this bp conformation is very short, as expected; i.e., the U·C bp decays rapidly. The situation is different for the adenosine bulge system. The correlation plot indicates a partially stable RC6·RG13 bp and hydrogen bonding between RA5·RG13. Most of the snapshots exhibit a bifurcated (RC6·RG13)·RA6 base triple, i.e., the canonical C·G bp is not completely broken (Fig. 3).

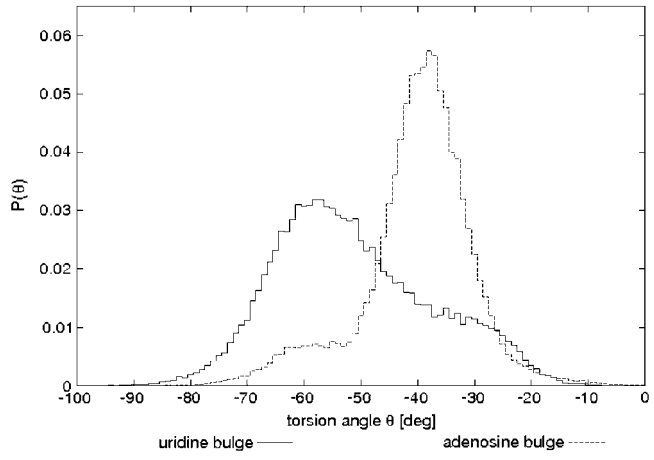

FIGURE 2 Probability distribution of dihedral angle θ for unrestrained bulge simulations in stacked conformation with a bin width of 1°.

The correlation plot of the A·G bp formation with respect to the torsion angle θ (Fig. 4) indicates a restricted flexibility of the adenine base when it participates in the base triple. The formation of an A·G bp with a hydrogen bond distance of 1.9 Å to 2.5 Å restricts the torsion angle θ in the range of $-50°$ to $-30°$. The disruption of this non-WC bp and the formation of a classical conformation (WC bp and stacked extra adenine) lead to a shift of θ to more negative values.

Based on the probability distributions P(θ) of the unrestrained MD simulations, the minimum in free energy for the stacked conformation in both bulge systems is predicted to be at $\sim -60°$ and $-40°$ for the uridine and the adenosine bulge system, respectively.

Potential of mean force for the bulge base looping out to the minor groove

The unrestrained MD simulations indicate that the bulge bases are significantly more mobile on the nanosecond timescale compared to bases involved in a regular WC bp. The potential of mean force for the bulge looping out process was investigated using umbrella sampling with a quadratic restraining potential for the dihedral angle θ (see Materials and Methods). Investigations on the convergence of the PMF with respect to the simulation time per sampling window revealed that a simulation time of 2 ns per window resulted in reasonable convergence (Fig. 5). Interestingly, the PMF converges rapidly for $\theta_{ref} = -40°$ up to $\theta_{ref} = 60°$ (in this range of θ the bulge base is still in contact with the RNA stem structure) but requires more sampling (2 ns per window) for the looped out and solvent exposed bulge structures ($\theta_{ref} \geq 60°$).

The potential of mean force for the complete bulge base looping out process starting from the final structure of the unrestrained simulations along the reaction coordinate θ is shown in Fig. 6. The free energy profiles for both uridine and adenosine bulges exhibit a wide low free energy region covering a range of more than 30° for the bulge systems adopting a stacked conformation. The minimum in free energy of the uridine bulge in stacked state is located at $-44°$, which is close but does not exactly correspond to the maximum of the probability distribution P(θ) of the relaxed and unrestrained structure. However, the free energy at that point ($\theta = -57°$) is <0.25 kcal mol^{-1} higher. The adenosine bulge RNA in stacked conformation has its minimum in free energy at $\theta = -40°$, which is in exact agreement with the expectation from the torsion angle distribution of the unrestrained

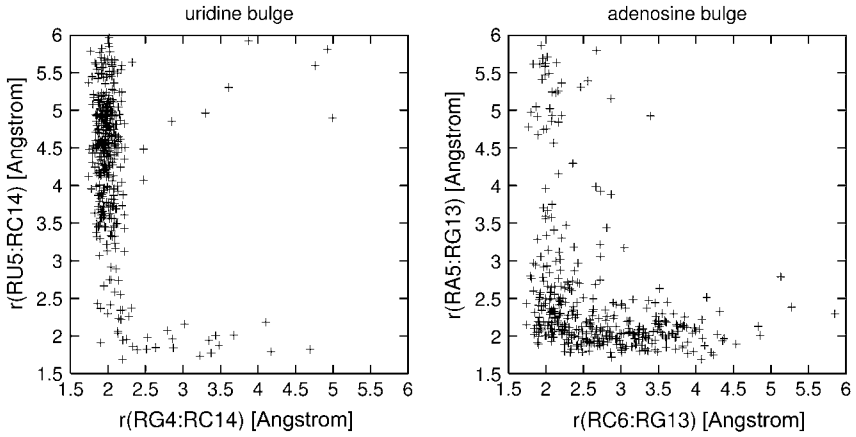

FIGURE 3 Bulge base hydrogen bonding interactions with flanking bps during unrestrained simulations starting from stacked bulge structures. The distance RU5.O4–RC14.1H4 has been plotted versus RG4.H1–RC14.N3 during the uridine bulge unrestrained simulations. The distance RA5.H61–RG13.O6 has been plotted versus RC6.H41–RG13.O6 during the unrestrained adenosine bulge simulations.

simulation. The bulge base looping out toward the major groove, i.e., more negative values of θ, leads to a plateau in free energy, which is at $\theta \approx -60°$ only 0.5 kcal mol^{-1} higher than at $\theta = -40°$.

Looping out of the uridine bulge to the minor groove (increasing values of θ) starting from the stacked state results in an increase in free energy, which can be explained by the introduction of tensions in the RNA backbone of the bulge-containing strand and a decreasing RG4/RU5 base stacking. The PMF reaches a maximum at $\theta = -5°$, which is associated with a structural change in the bulge region of the molecule. This transition state is ~3.7 kcal mol^{-1} higher in free energy than the initial state. The bulge base slides out of the helical stack and a hydrogen bond is established between RG4.H21 (NH_2 group) and RU5.O4, i.e., a RG4·RC14·RU5 base triple is formed (Fig. 7). Interestingly, an analogous base triple has been observed by other authors using MD simulations with a single uracil bulge base establishing an RA.H6-RU.O4 hydrogen bond to its 5′ flanking A·U bp in the minor groove (25). The base triple conformation relaxes by further looping out, reaching a minimum in free energy at $\theta = 25°$, which is even lower than the initial stacked conformation by ~1 kcal mol^{-1}. The base triple is stable up to $\theta \sim 60°$. Further looping out releases the bulge base to the minor groove to become completely solvent exposed. The PMF then maintains a constant level of $\Delta G \approx 5.5$ kcal mol^{-1} with respect to the initial stacked conformation.

Looping out the adenine bulge base results in a qualitatively similar PMF profile. The adenine base slides out to the minor groove at $\theta \sim -7°$ and forms a base triple with the 5′ flanking bp. However, in contrast to the uridine bulge this base triple has a completely planar geometry (Fig. 8; in the case of the uracil bulge base, the bulge base is in a tilted orientation relative to the adjacent bp; Fig. 7). The barrier between stacked and triple state is ~3 kcal mol^{-1}, slightly lower than the corresponding transition state of the uridine bulge system. In contrast to the equivalent barrier in the case of the uridine bulge, it has a shoulder located at $\theta = -15°$.

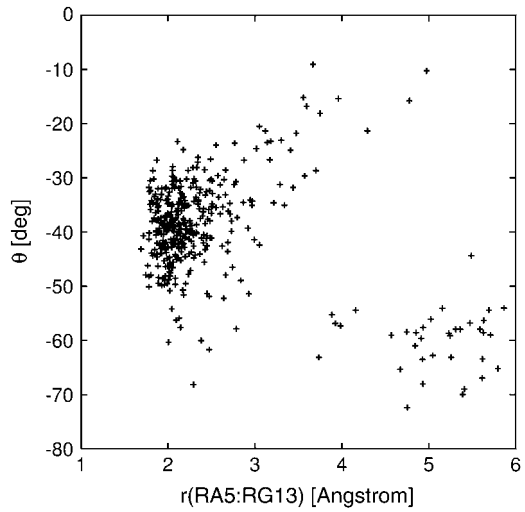

FIGURE 4 Correlation between RA5.H61–RG13.O6 hydrogen bond length and torsion angle θ during unrestrained adenosine bulge simulations.

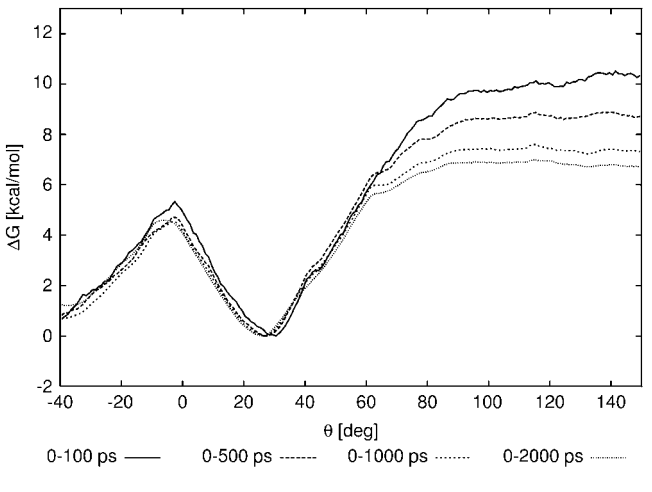

FIGURE 5 Convergence of the potential of mean force calculations on uridine bulge with respect to sampling interval (data gathering time is given after 50 ps equilibration during each 5° step in the dihedral angle θ).

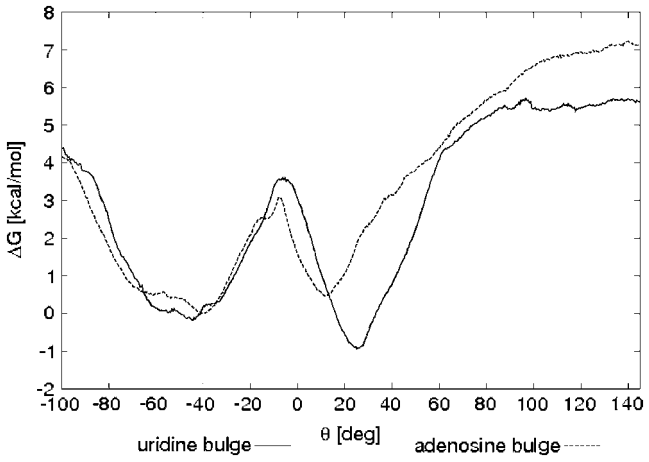

FIGURE 6 Potential of mean force (2 ns data gathering per 5° step) for uridine and adenosine bulge base looping out along the reaction coordinate θ.

This shoulder arises from the formation of an intermediate hydrogen bond between RA5.H62 and RC14.O2 as well as by interbase stacking between RA5 and RC6. The coplanar orientation of the adenine bulge base in the triple base with the adjacent RG4·RC14 bp allows the formation of hydrogen bonds to both the guanine and the cytosine base with an average bond length of r(RA5.N7–RG4.H21) = 2.0 Å and r(RA5.H61–RC14.O2) = 2.2 Å, respectively. This bulge conformation has its minimum in free energy at $\theta = 15°$ and is ~0.5 kcal mol^{-1} higher than the stacked conformation. Further looping out results in an increase of the calculated PMF. The base triple is retained up to 40° and then the adenine bulge base is released toward the minor groove. The completely looped out conformation of the adenosine bulge RNA molecule is ~7 kcal mol^{-1} higher in free energy than the initial stacked conformation. This result indicates that in the case of an extra adenosine bulge the full looping out requires ~1.5 kcal mol^{-1} more free energy than the same process in the case of a uridine bulge.

Evolution of the backbone conformation

The bulge base looping out process is also accompanied by conformational rearrangements of the RNA backbone at the bulge nucleotide itself as well as at the 5′ flanking nucleotide. Fig. 9 shows the average values of the six backbone torsion angles of the bulge nucleotides and their flanking nucleotides.

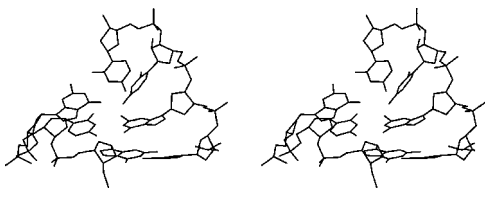

FIGURE 7 Stereo view of the uridine bulge (simulation snapshot) located in the minor groove forming a base triple with the 5′ flanking bp during the PMF simulations at $\theta_{ref} = 25°$.

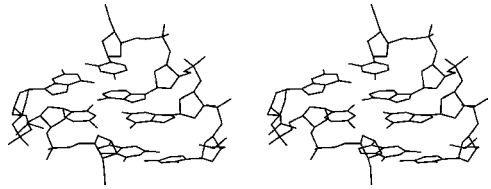

FIGURE 8 Stereo view of the adenosine bulge forming a base triple with the 5′ flanking bp in the minor groove during the PMF simulations of the adenosine bulge system at $\theta_{ref} = 15°$.

The conformational changes in the RNA backbone at the bulge sites are accompanied by a slight decrease of γ_5 as well as of ε_5 and ζ_5 (backbone torsion angles at the bulge nucleotide) in going from the stacked conformation to the base triple, due to the coaxial rotation of the ribose sugar ring of the bulge nucleotides. The key backbone torsion angle change appears to be the increase in ε_5 since it is seen in both the uridine and adenosine bulge cases. The result indicates that partial looping out and formation of a base triple in the minor groove does not require major changes in the nucleic acid backbone structure. However, at values of $\theta \approx 65°$, when the base triple disrupts and the bulge base is released the normal vector of the ribose mean plane alters from a perpendicular to a parallel orientation with respect to the helical axis. The full looping out process is accompanied by a concerted rise of ε_5 and a drop of ζ_5. In addition, the bulge nucleotide ribose rings change their sugar pucker from the C3′ endo to the C2′ endo conformation, indicated by the rise of δ_5 (Fig. 9). The torsion angle α_5 changes transiently from the $-g$ to the $+g$ regime. Interestingly, in the case of the looped out adenine bulge base ($\theta > 80°$) one can also observe both a change in the ε_4 torsion angle and the ribose pucker toward a C2′ endo state one nucleotide before the bulge site.

The conformational changes are not restricted to the bulge nucleotide alone. The backbone of the 5′ flanking nucleotide is also affected by the bulge base looping out process. In particular, the torsion angles ε and ζ change their regime that reveals a flip over of the phosphate linker group orientation. Furthermore, the sugar pucker of the adjacent guanosine (nucleotide 4) switches from the C3′ endo to the C2′ endo conformation in the case of the uracil bulge base looping out. The observed α/γ flips at the 5′ uridine adjacent nucleotide do not interfere with the dihedral angle θ and thus do not affect the free energy profile. Since in each step of the looping out simulation a set of three consecutive windows is sampled at once, the entire looping out path is accomplished within a few nanoseconds of MD simulation and does not exceed the average lifetime of the flipped α/γ conformation. Hence, a relaxation or even frequent transitions were not observed during these studies.

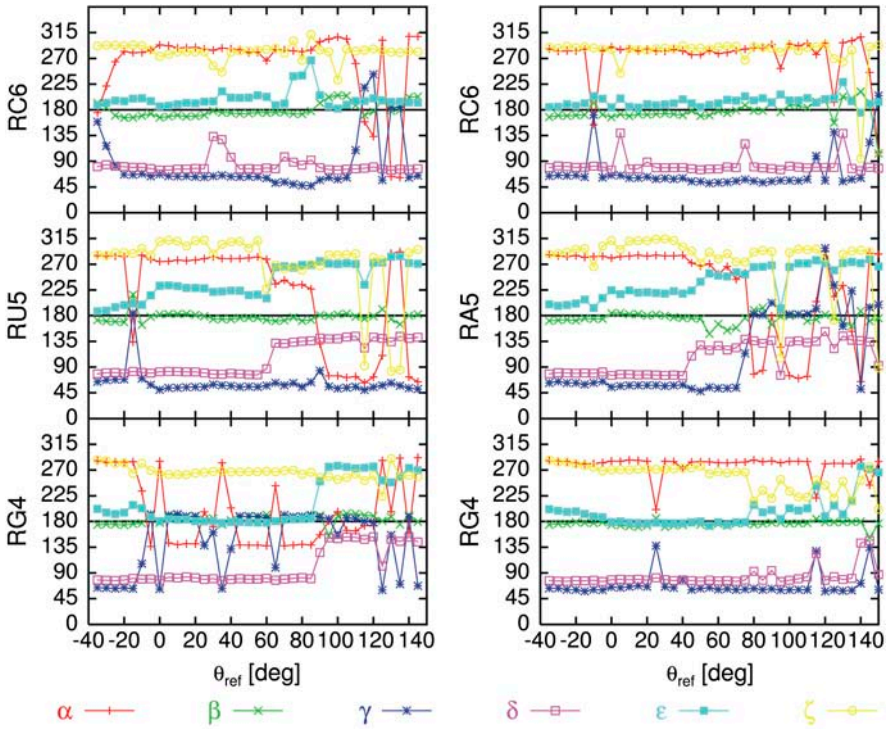

FIGURE 9 Mean values of backbone torsion angles for RC6 (*top*), RU5/RA5 (*center*), and RG4 (*bottom*). (*Left panels*) Uridine bulge system. (*Right panels*) Adenosine bulge system. Negative values of torsion angles ω have been converted by $360° + \omega$ to get a range $0° \leq \omega \leq 360°$.

The comparison of the structures at the final sampling window, i.e., $\theta = 145°$, shows different backbone conformations at the bulge sites. However, key features observed in both looped out adenosine and uridine bulges are a concerted change of ε and ζ at the bulge nucleotides as well as a transition of the bulge and 3′-neighboring nucleotide sugar pucker toward C2′-endo states (the transition at the neighboring nucleotide was only partially seen in the case of the adenosine bulge structure). Very similar backbone conformations have been observed in experimental structures of looped out extra nucleotides (14). The obtained final conformations of the adenosine and the uridine bulge site are very close to experimental structures, as demonstrated by the superposition of a snapshot from the simulation and the experimental structure of the MS2 phage adenosine bulge (15,54; Fig. 10).

Helical parameters of initial and final states

The helical parameters for the bulge systems in stacked as well as in looped out conformation were calculated from the trajectories at $\theta_{ref} = -35°$ and $+145°$ using the program Curves (40,41). Most of the average helical bp parameters were not significantly affected by the presence of the central bulge nucleotide compared to a simulation of the dsRNA reference structure. Note, that the Curves analysis of the bulge-containing molecules only concerns the helical parameters of the bps (the bulge base is not included).

As expected the presence of the bulge base in the stacked form affects the rise and twist between flanking bps. Interestingly, the increase in rise is localized to the step between bulge flanking bps but also affects the next nearest neighboring bp steps in the case of the uridine bulge. For both bulge cases an ''overtwisting'' of the step formed by the bps flanking the bulge was observed, whereas a reduced twist of the next bp step was found (Figs. 11 and 12). The bulge also results in an increased tilt of the central bp step.

For the looped out conformation of both bulge systems, the situation is different. The base-base as well as the interbasepair parameters of the adenosine bulge RNA are in good agreement with those of the parent RNA molecule (Fig. 12). This includes rise and twist of bps flanking the bulge nucleotide as well as the average roll and twist angles. The uridine

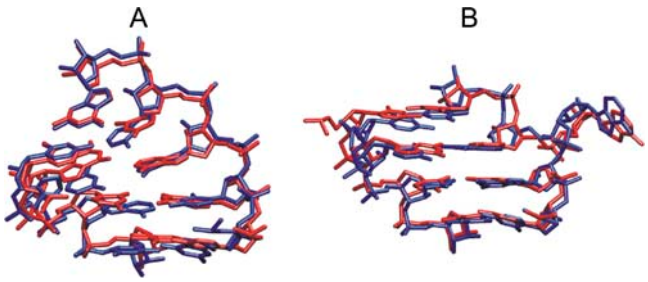

FIGURE 10 Superposition of experimental (*blue*) and simulated (*red*) adenosine bulge structures with respect to the C1′ atoms of the bps. (*A*) Snapshot from a simulation in the stacked state compared to an experimental stacked adenosine bulge; Protein Data Bank code 17RA (54). (*B*) Snapshot from a fully looped out bulge state ($\theta_{ref} = 145°$) compared to the experimental structure of a single adenosine bulge of the phage MS2 RNA operator; Protein Data Bank code 1E6T (63).

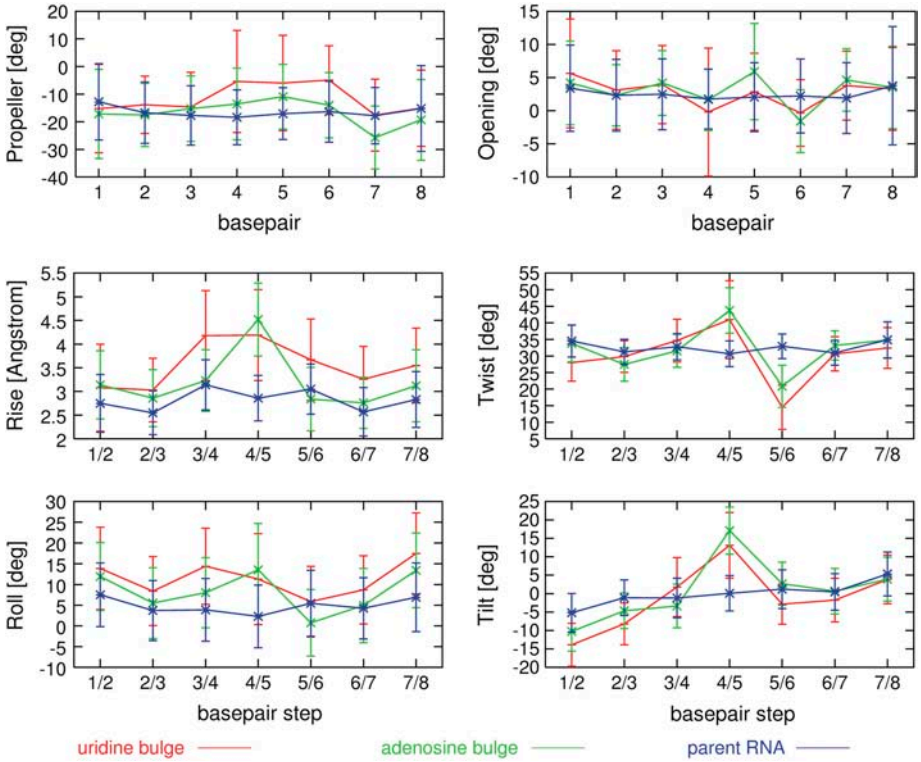

FIGURE 11 Averaged helical bp and base step parameters of uridine (*red*) and adenosine (*green*) bulged RNA in stacked conformation as well as of canonical dsRNA (*blue*) as reference.

bulge RNA has slightly different properties in the looped out conformation than the adenosine bulge RNA. One reason is the different backbone conformation around the bulge nucleotide, which results in an insufficient bp stacking of both bulge flanking bps. A small increase of twist and tilt angles at the bulge bp step and a local undertwisting at the subsequent bp step as well as a shift of rise in the bulge adjacent bp step was observed compared to the regular helix.

Energetics of the looping out process using the MM-GBSA approach

The umbrella sampling method allows us to calculate the potential of mean force or free energy change along the looping out reaction coordinate including energetic as well as entropic contributions. To get an impression on the various energetic contributions to the process MM-GBSA were performed (46,48). The analysis was performed on the recorded trajectories (only solute coordinates) of the sampling windows with 200 frames per window. The potential energy was averaged over the trajectory and decomposed into its energetic contributions. The nonbonded energy contributions, e.g., van der Waals, Coulomb, and generalized Born energy are of particular interest. To reduce the influence of fluctuations due to interactions far away from the bulge site, the MM-GBSA approach was applied to the core region of the RNA molecules; i.e., the bulge nucleotides and the flanking bps were extracted from the trajectories. The resulting average MM-GBSA energy contributions still showed considerable fluctuations between neighboring simulation trajectories. Nevertheless, clear trends to estimate energetic contributions for stacked, intermediate triple and fully looped bulge conformations can be extracted. The results of the MM-GBSA calculations (Figs. 13 and 14) roughly reflect the PMF profile generated by the umbrella sampling. The profiles of the potential energy and the nonbonded energies can be divided into three regimes representing the stacked, the intermediate base triple, and the looped out conformation.

For the uridine bulge RNA, the potential energy rises in going from the first to the second regime, i.e., when the bulge base slides out of the helical stack to form the base triple with the adjacent bp. The van der Waals energy is reduced due to the loss of base stacking interaction upon slide out of the base. The base triple formation results in a decrease of both the potential energy and the van der Waals energy. After crossing a barrier of $\sim$6 kcal mol^{-1} with respect to the stacked state, the potential energy is even lower in the base triple conformation than for the initial stacked state (by $\sim$2 kcal mol^{-1} compared to $\sim$1 kcal mol^{-1} found in the PMF calculation). The barrier height is similar to the barrier height obtained during the PMF calculation ($\sim$4 kcal mol^{-1}). The intermediate base triple structure is stabilized by electrostatic interactions but has a slightly higher van der Waals energy compared to the stacked state. At $\theta \approx 60°$, when the base triple breaks, the total energy and especially the van der Waals energy and nonpolar surface area dependent contribution increase. The electrostatic energy (sum of Coulomb and generalized Born (GB) solvation energy) increases when

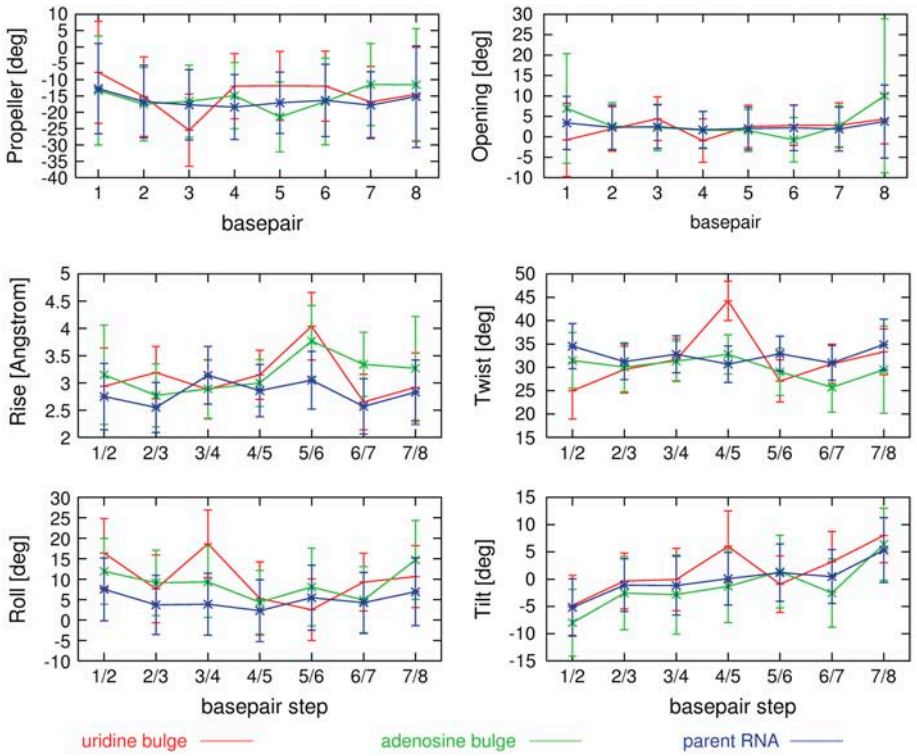

FIGURE 12 Averaged helical bp and base step parameters of adenosine (*red*) and adenosine (*green*) bulged RNA in looped out conformation as well as of canonical parent RNA (*blue*) as reference.

the bulge base slides out and contributes together with the van der Waals term to the energy barrier for looping out of the bulge base. The base triple formation results in a decrease of electrostatic energy, i.e., a stabilization of the structure, due to the formation of a new hydrogen bond and more favorable electrostatic solvation. The electrostatic energy decreases further when the base triple breaks at $\theta = 60°$. The total calculated MM-GBSA energy difference between stacked and looped out uracil structures was ~7 kcal mol^{-1}, slightly larger than the calculated PMF free energy difference (5.5 kcal mol^{-1}).

The adenine base looping out exhibits qualitatively similar features in the energy profiles as observed for the uracil

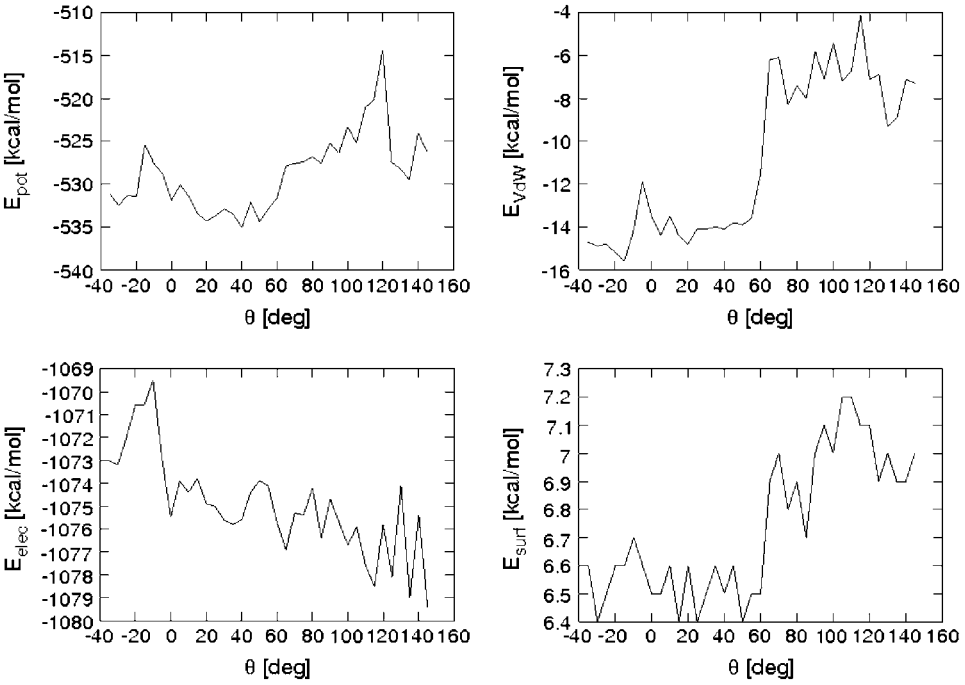

FIGURE 13 MM-GBSA energies of the bulge nucleotide and flanking bps: total potential energy (E_{pot}: *upper left panel*) and its contributions from van der Waals (E_{vdW}: *upper right panel*), electrostatic (E_{elec}: Coulomb + GB solvation; *lower left panel*), and nonpolar surface area dependent contribution (E_{surf}: *lower right panel*) of uracil bulge base looping out.

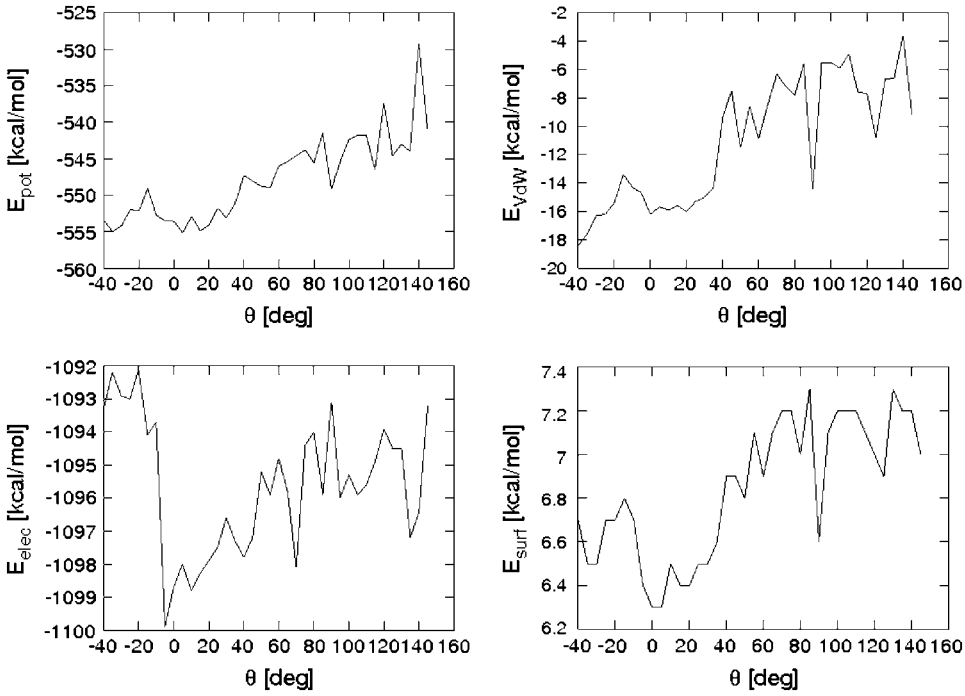

FIGURE 14 Same as in Fig. 13 for the adenine bulge base looping out.

bulge base. Again one can distinguish two low energy regimes. In this case the lowest energy regime represents the bulge stacked state separated from a second low energy regime representing the minor groove triple state. Interestingly, similar to the calculated PMF the stacked state MM-GBSA energy is slightly lower ($\sim$0.5 kcal mol^{-1}) than the minor groove triple state. Also, the barrier energy height separating the stacked and triple states appears to be slightly smaller ($\sim$4 kcal mol^{-1}) than for the uridine bulge, which was also found for the PMF profiles. The fully looped out regime ($\theta > 60°$) differs in total energy by $\sim$9 kcal mol^{-1} from the stacked state (Fig. 14). Interestingly, the electrostatic contribution strongly stabilizes the triple state and in contrast to the uracil looping out process, the electrostatic energy increases beyond $\theta = 70°$, when the adenine base becomes completely solvent exposed. Consistent with the results from the PMF calculations, looping out of the uracil bulge is predicted to be more favorable by $\sim$2 kcal mol^{-1} compared to looping out of an adenine bulge.

Further looping out and flipping toward the major groove

To obtain a full cycle of bulge base looping, we attempted to loop the bulge bases in the looped out conformations ($\theta_{ref} = 145°$) further toward the major groove. However, further increase of the dihedral angle θ resulted in conformations with the vectors RB5.N1(N9)-RB5.C1′ and RB5.C1′-RC6.C1′, which determine the dihedral angle θ, becoming colinear and remaining trapped in this conformation. This observation indicates that the pseudodihedral angle θ is not useful to loop out the bulge base beyond θ values above $\sim$150°.

We also tried to loop out the bulge bases from the initial conformation toward the major groove starting from sampling window $\theta_{ref} = -35°$. Looping out along the major groove pathway includes passing the bulge nucleotide ribose unit through the helical stem. The movement of the polar sugar through the intrahelical space between the helical stems was unfavorable and lead to a disruption of the flanking bps at $\theta_{ref} = -80°$ and also changes of the backbone at the complementary strand. Disruption of the flanking bps could not be prevented by including restraints to keep the flanking bps in a paired geometry during an equilibration phase. It occurred in both bulge RNAs and was independent of the starting structure and simulation time. Further looping out did not lead to a ''reclosure'' of flanking bps. Our conclusion from this result is that the barrier of bulge looping out to the major groove appears to be considerably higher than looping out to the minor groove. The forced movement of the bulge base and the ribose sugar through the narrow cleft between the flanking bps leads to major conformational changes that do not relax on the timescale of our simulations.

DISCUSSION

Extra unmatched bulge bases are frequently found in folded RNA molecules and often participate in RNA-ligand as well as tertiary interactions (6,8,9). Structural and molecular modeling studies of single base bulges indicate that this motif can adopt a variety of conformations and can change its conformation upon ligand binding (14–16,55–57). In this study, explicit solvent MD simulations have been used to study the dynamics of uridine and adenosine bulges in RNA and compare it with the dynamics of regular dsRNA. In the

unrestrained simulations on the bulges starting from intrahelical stacked conformations, both adenine and uracil bulge bases showed larger mobility than bases involved in WC bps and formed temporary non-WC bps or bifurcated bps to flanking bases on the opposite strand. However, no spontaneous transition to a looped out conformation was observed, indicating a barrier to slide out of the stacked state.

In addition, the process of single bulge base looping out along the minor groove pathway was studied by applying the umbrella sampling method using a pseudodihedral angle as reaction coordinate supplemented with MM-GBSA studies on the generated conformers. The calculated free energy profiles for the forced uracil and adenine looping out process exhibited similar characteristics. A broad low free energy region around the stacked initial conformation was found which agrees with the broad probability distribution of the dihedral angle θ observed during unrestrained simulations. This also agrees with previous MD studies on other bulge systems (25,26) and NMR studies (58) that indicate larger mobility of bulge bases even in the stacked intrahelical state. Looping out to the minor groove lead to the sliding out of the bulge base from the helical stack. This sliding out is accompanied with a decrease of stacking interactions and an increase in backbone tension that causes an increase in free energy. Further looping out passes an energy barrier and enables the formation of intermediate base triples with the 5′ flanking bp, which are very stable over a range of $\theta = 40$–$60°$. In the case of the extra uracil, this conformation was found to be more stable than the stacked intrahelical bulge conformation. Interestingly, this result agrees with an NMR structure of a single uracil bulge in the P4 element from bacterial RNase P that also indicates an extrahelical bulge base contacting the RNA minor groove (59). Interestingly, in a recent MD study of the concerted breaking of a bp in RNA and looping out of an adenine base, a second local free energy minimum (besides the stacked and basepaired state) was also found with the adenine base located in the minor groove (60). When the base triple conformations were broken upon further looping out, the bulge bases become fully solvent exposed without contacts to the RNA. This event was accompanied by characteristic changes in the nucleic acid backbone; e.g., ribose pucker has changed from the C3′ endo to C2′ endo conformation at the bulge and the 3′-neighboring nucleotide and concerted changes in the ε and ζ torsion angles. Similar backbone conformations have been described in x-ray structures of looped out single adenosine bulges in A-form RNA/DNA hybrids (14) and have been found in previous conformational analysis studies of single base bulges (56). The final fully looped out conformation of the adenosine bulge also showed close agreement (in terms of atomic Rmsd) with the single adenosine bulge x-ray structure of the phage MS2 RNA (15).

For both the uridine as well as the adenosine bulge, the PMF calculations predicted a positive free energy change of 5.5 and 7 kcal mol^{-1}, respectively, for the fully looped out versus stacked conformation. A positive free energy change is expected due to the loss of bulge base stacking interactions as well as by the solvent exposure of the hydrophobic bulge bases. Since the adenine base interacts more strongly with the bulge flanking bps and is more hydrophobic, the free energy difference between stacked and looped out states is larger than for the uracil bulge base. In the case of the adenosine bulge, the calculated preference of the stacked state agrees with the observation that in solution single adenosine bulges tend to adopt a stacked intrahelical conformation (55). However, conformations with the adenine bulge base contacting the RNA minor groove have also been observed, for example, for a uracil to adenine mutation of the single base bulge of the P4 stem of RNase P (61). In the case of the uridine bulge, extrahelical structures have been found, however, often with the bulge base still contacting the RNA helix (59), agreeing qualitatively with this study of a stable extrahelical uracil base contacting the RNA in the minor groove. When comparing the calculated free energy changes with an experimentally observed equilibrium of stacked versus looped out bulge conformers, it is important to keep in mind that looped out forms represent an ~4 times larger range of conformers with respect to the present reaction coordinate than stacked bulge structures (see Fig. 6). This larger conformational range of looped out forms lowers the effective free energy difference between stacked and (any) looped out form by ~1 kcal mol^{-1}. As expected the calculated free energy for looping out of a bulge base is smaller than results obtained for the combined breaking of a bp and subsequent looping out one base (32,33,60,62). Depending on the type of bp in DNA (32,33,62) and RNA (32,60), free energy changes of 10–23 kcal mol^{-1} were found. It should be emphasized that the free energy difference associated with the looping out of a bulge base might depend considerably on the sequence context. Both the bulge base interaction with neighboring bps in the intrahelical stacked state as well as the stacking interaction of neighboring bases in the looped out state will influence the free energy difference. It is also likely that the stability of intermediate states (e.g., base triples) depends on the surrounding sequence. A systematic analysis of the sequence context dependence is possible in future studies by performing free energy calculations of bulge base looping in different sequence environments.

MM-GBSA calculations based on the recorded trajectories showed significant variations between neighboring simulation windows, however, reflected the characteristics of the looping out process obtained from the PMF calculations qualitatively well. The calculated MM-GBSA energy differences between looped out and stacked bulge conformations were slightly larger than the corresponding free energy differences from the PMF calculations. This is expected since the higher conformational entropy (mobility) in the looped out states (not accounted for in the MM-GBSA calculations) stabilizes the looped out state, resulting in a lower PMF free energy difference between stacked and looped out forms

compared to the MM-GBSA results. The MM-GBSA calculations indicated that electrostatic interactions overall favor the looped out and base triple structures, whereas van der Waals and nonpolar solvation contributions strongly favored the stacked state.

For large values of the dihedral angle θ (fully looped out bulge structures), the problem of a co-linear arrangement of the vectors that determine the dihedral angle was observed. This observation points to a limitation of the range of useful values of the dihedral angle θ as a reaction coordinate to drive the looping out of the bulge bases. This effect has so far not been described in base flipping studies of regular bps in DNA or RNA using similar (but not identical) dihedral angle reaction coordinates (33,60,62).

In addition, the looping out toward the major groove (starting from stacked structures) lead to significant structural changes including a disruption and opening of bulge flanking bps. The pathway toward the major groove involves the ribose of the bulge nucleotide to slide through the narrow space of the two flanking bps and introduces mechanical stress into the strands. Sterical interactions and strong hydrogen bonding interactions of the ribose 2′-OH group with the O4′ of the bulge flanking ribose formed during the looping out toward the major groove are the likely reasons for the observed perturbation of bulge flanking bps. A conclusion from this result is the prediction of a higher barrier for looping out of bulge bases in RNA toward the major groove than toward the minor groove. The molecular mechanism of bp disruption and subsequent base flipping out of the helix has been investigated by several groups using MD simulations applying the umbrella sampling method (29,30,32,33,60,62). Interestingly, in the case of the combined bp breaking and base looping out PMF calculations, the perturbation of flanking bps upon flipping toward the major groove has not been observed. In the case of B-DNA the major groove base flipping pathway was found to be the more favorable pathway (32). However, in a recent study of bp breaking and base flipping in A-RNA, the minor groove pathway was found to be more favorable than major groove looping out (60). An important difference between bulge base flipping out and combined bp breaking and base flipping is the presence of a base opposite of the flipped base in the latter process. The base in the opposite strand keeps a larger space between the bps that flank the flipped base, allowing the ribose to easily slide through the helical structure. The absence of such a ''space holder'' on the opposite strand in the case of single base bulges results in a much narrower space and limits the motion of the ribose toward the major groove.

CONCLUSIONS

Extra unmatched bulge bases are important RNA structural motifs that can mediate tertiary interactions and participate in drug and protein binding. Such binding and recognition events can involve conformational changes in the bulge motif. An estimate of associated free energy changes to loop out a bulge base or to reach stable substates is important to better understand its contribution to binding and tertiary structure formation. The current comparative simulation study on the process of looping or flipping out an extra adenine and an uracil bulge base in RNA allowed us to estimate the corresponding change in free energy, to characterize energy barriers and stable intermediate substates, and to characterize energetic contributions to the process. Overall good agreement of the starting and final structures of the looping out process with available experimental data was observed. The calculated free energy penalty for looping out starting from stacked states was larger for an adenosine versus uridine bulge and revealed stable substates of similar free energy with the bulge bases located in the minor groove forming triple-like pairing geometries. A transition barrier of ~3–4 kcal mol^{-1} was obtained for the sliding out of the bulge base toward the minor groove. This barrier is significantly above RT (gas constant times temperature) at room temperature but indicates that occasional spontaneous flipping between stacked and partially looped out states is possible. The calculations also indicate that flipping out of bulge bases toward the minor groove appears to be more favorable than flipping toward the major groove.

We thank Drs. D. Roccatano and N. Riemann for helpful discussions.

This work was performed using the computational resources of the Computer Laboratories for Animation, Modeling and Visualization at International University Bremen and supercomputer resources of the Environmental Molecular Science Laboratories at the Pacific Northwest National Laboratories (grant gc11-2002).

REFERENCES

1. Moore, P. B. 1999. Structural motifs in RNA. *Annu. Rev. Biochem.* 68:287–300.
2. Zacharias, M. 2000. Simulation of the structure and dynamics of non-helical RNA motifs. *Curr. Opin. Struct. Biol.* 10:307–311.
3. Hall, K. B. 2002. RNA-protein interactions. *Curr. Opin. Struct. Biol.* 12:283–288.
4. Ferre-D'Amare, A. R., and J. A. Doudna. 1999. RNA folds: insights from recent crystal structures. *Annu. Rev. Biophys. Biomol. Struct.* 28: 57–73.
5. Leontis, N. B., and E. Westhof. 2003. Analysis of RNA motifs. *Curr. Opin. Struct. Biol.* 13:300–308.
6. Egli, M. 2004. Nucleic acid crystallography: current process. *Curr. Opin. Chem. Biol.* 8:580–591.
7. Schroeder, R., A. Barta, and K. Semrad. 2004. Strategies for RNA folding and assembly. *Nat. Rev. Mol. Cell Biol.* 5:908–919.
8. Turner, D. H. 1992. Bulges in nucleic acids. *Curr. Opin. Struct. Biol.* 2:334–337.
9. Gutell, R. R., J. J. Cannone, Z. Shang, Y. Du, and M. J. Serra. 2000. A story: unpaired adenosine bases in ribosomal RNAs. *J. Mol. Biol.* 304: 335–354.
10. Nikonowicz, E., R. P. Meadows, and D. G. Gorenstein. 1990. NMR structural refinement of an extra-helical adenosine tridecamer d(CGCAGAATTCGCG)$_2$ via hybrid relaxation matrix procedure. *Biochemistry.* 29:4193–4204.

11. Weeks, K. M., and D. M. Crothers. 1993. Major groove accessibility of RNA. *Science*. 261:1574–1577.
12. Gohlke, C., A. I. H. Murchie, D. M. J. Lilley, and R. M. Clegg. 1994. Kinking of DNA and RNA helices by bulge nucleotides observed by fluorescence energy transfer. *Proc. Natl. Acad. Sci. USA*. 91:11660–11664.
13. Zacharias, M., and P. J. Hagerman. 1995. Bulge-induced bends in RNA: quantification by transient electric birefringence. *J. Mol. Biol*. 247: 486–500.
14. Portmann, S., S. Grimm, C. Workman, N. Usman, and M. Egli. 1996. Crystal structures of an A-form duplex with single-adenosine bulges and conformational basis for site-specfic RNA self-cleavage. *Chem. Biol*. 3:173–184.
15. Valegard, K., J. B. Murray, P. G. Stockely, N. J. Stonehouse, and L. Liljas. 1994. Crystal structure of an RNA bacteriophage coat protein-operator complex. *Nature*. 371:623–626.
16. Puglisi, J. D., L. Chen, S. Blanchard, and A. D. Frankel. 1995. Solution structure of a bovine immunodeficiency virus Tat-TAR peptide-RNA complex. *Science*. 270:1200–1203.
17. Aboul-ela, F., J. Karn, and G. Varani. 1996. Structure of HIV-1 TAR RNA in the absence of ligands reveals a novel conformation of the trinucleotide bulge. *Nucleic Acids Res*. 24:3974–3981.
18. Puglisi, J. D., R. Tan, B. J. Calnan, A. D. Frankel, and J. R. Williamson. 1992. Conformation of the TAR RNA-arginine complex by NMR spectroscopy. *Science*. 257:76–80.
19. Puglisi, J. D., L. Chen, A. D. Frankel, and J. R. Williamson. 1993. Role of RNA structure in arginine recognition of TAR RNA. *Proc. Natl. Acad. Sci. USA*. 90:3680–3684.
20. Ippolito, J. A., and T. A. Steitz. 1998. A 1.3-Å resolution crystal structure of the HIV-1 trans-activation response region RNA stem reveals a metal ion-dependent bulge conformation. *Proc. Natl. Acad. Sci. USA*. 95:9819–9824.
21. Long, K. S., and D. M. Crothers. 1999. Characterization of the solution conformations of unbound and Tat peptide-bound forms of HIV-1 TAR RNA. *Biochemistry*. 38:10059–10069.
22. Witherell, G. W., J. M. Gott, and O. C. Uhlenbeck. 1991. Specific interaction between RNA phage coat proteins and RNA. *Prog. Nucleic Acid Res. Mol. Biol*. 40:185–220.
23. Wu, H.-N., and O. C. Uhlenbeck. 1987. Role of a bulged A residue in a specific RNA protein interaction. *Biochemistry*. 26:8221–8227.
24. Cheatham, T. E. 2004. Simulation and modeling of nucleic acid structure, dynamics and interactions. *Curr. Opin. Struct. Biol*. 14:360–367.
25. Sarzynska, J., T. Kulinski, and L. Nilsson. 2000. Conformational dynamics of a 5S rRNA hairpin domain containing loop D and a single nucleotide bulge. *Biophys. J*. 79:1213–1227.
26. Feig, M., M. Zacharias, and M. E. Pettitt. 2001. Conformation of an adenine bulge in a DNA octamer and its influence on DNA structure from molecular dynamics simulations. *Biophys. J*. 81:352–370.
27. Roberts, R. J., and X. Cheng. 1998. Base flipping. *Annu. Rev. Biochem*. 67:181–198.
28. Giudice, E., P. Várnai, and R. Lavery. 2001. Energetic and conformational aspects of A:T base-pair opening within the DNA double helix. *ChemPhysChem*. 11:673–676.
29. Giudice, E., P. Várnai, and R. Lavery. 2003. Base pair opening within B-DNA: free energy pathways for GC and AT pairs from umbrella sampling simulations. *Nucleic Acids Res*. 31:1434–1443.
30. Várnai, P., and R. Lavery. 2002. Base flipping in DNA: pathway and energetics studied with molecular dynamic simulations. *J. Am. Chem. Soc*. 124:7272–7273.
31. Giudice, E., and R. Lavery. 2002. Simulations of nucleic acids and their complexes. *Acc. Chem. Res*. 35:350–357.
32. Giudice, E., and R. Lavery. 2003. Nucleic acid base pair dynamics: the impact of sequence and structure using free-energy calculations. *J. Am. Chem. Soc*. 125:4998–4999.
33. Huang, N., N. K. Banavali, and A. D. MacKerell Jr. 2003. Protein facilitated base flipping in DNA by cytosine-5-methyltranferase. *Proc. Natl. Acad. Sci. USA*. 100:68–73.
34. Pan, Y., and A. D. MacKerell Jr. 2003. Altered structural fluctuations in duplex RNA versus DNA: a conformational switch involving base pair opening. *Nucleic Acids Res*. 31:7131–7140.
35. Huang, N., and A. D. MacKerell Jr. 2004. Atomistic view of base flipping in DNA. *Philos. Transact. A Math Phys. Eng. Sci*. 362:1439–1460.
36. Case, D. A., D. A. Pearlman, J. W. Caldwell, T. E. Cheatham III, W. S. Ross, C. L. Simmerling, T. A. Darden, K. M. Merz, R. V. Stanton, A. L. Cheng, J. J. Vincent, M. Crowley, V. Tsui, R. J. Radmer, Y. Duan, J. Pitera, I. Massova, G. L. Seibel, U. C. Singh, P. K. Weiner, and P. A. Kollman. 1999. AMBER 6. University of California, San Francisco.
37. Ryckaert, J.-P., G. Ciccotti, and H. J. C. Berendsen. 1977. Numerical integration of the Cartesian equations of motion of a system with constraints: molecular dynamics of n-alkanes. *J. Comput. Phys*. 23: 327–341.
38. Miyamoto, S., and P. A. Kollman. 1992. Settle: An analytical version of the SHAKE and RATTLE algorithm for rigid water models. *J. Comput. Chem*. 13:952–962.
39. Berendsen, H. J. C., J. P. M. Postma, W. F. van Gunsteren, A. DiNola, and J. R. Haak. 1984. Molecular dynamics with coupling to an external bath. *J. Chem. Phys*. 81:3684–3690.
40. Lavery, R., and H. Sklenar. 1988. The definition of generalized helicoidal parameters and of axis curvature for irregular nucleic acids. *J. Biomol. Struct. Dyn*. 6:63–91.
41. Lavery, R., and H. Sklenar. 1988. Defining the structure of irregular nucleic acids. *J. Biomol. Struct. Dyn*. 6:655–667.
42. Kumar, S., D. Bouzida, R. H. Swendsen, P. A. Kollman, and J. M. Rosenberg. 1992. The weighted histogram analysis method for free-energy calculations on biomolecules. I. The method. *J. Comput. Chem*. 13:1011–1021.
43. Roux, B. 1995. The calculation of the potential of mean force using computer simulations. *Comput. Phys. Commun*. 91:275–282.
44. Kobrak, M. N. 2003. Systematic and statistical error in histogram-based free energy calculations. *J. Comput. Chem*. 24:1437–1446.
45. Grossfield, A. 2003. http://dasher.wustl.edu/alan.
46. Srinivasan, J., J. Miller, P. A. Kollman, and D. A. Case. 1998. Continuum solvent studies of the stability of RNA hairpin loops and helices. *J. Biomol. Struct. Dyn*. 16:671–682.
47. Srinivasan, J., M. W. Trevathan, P. Beroza, and D. A. Case. 1999. Application of a pairwise generalized Born model to proteins and nucleic acids: inclusion of salt effects. *Theor. Chem. Acc*. 101:426–434.
48. Kollman, P. A., I. Massova, C. Reyes, B. Kuhn, S. Huo, L. Chong, M. Lee, Y. Duan, W. Wang, O. Donini, P. Cieplak, J. Srinivasan, D. A. Case, and T. E. Cheatham III. 2000. Calculating structures and free energies of complex molecules: combining molecular mechanics and continuum models. *Acc. Chem. Res*. 33:889–897.
49. Still, W. C., A. Tempczyk, R. C. Hawley, and T. Hendrikson. 1990. Semianalytical treatment of solvation for molecular mechanics and dynamics. *J. Am. Chem. Soc*. 112:6127–6129.
50. Hawkins, G. D., C. J. Cramer, and D. G. Truhlar. 1995. Pairwise solute descreening of solute charges from a dielectric continuum. *Chem. Phys. Lett*. 246:122–129.
51. Hawkins, G. D., C. J. Cramer, and D. G. Truhlar. 1996. Parametrized models of aqueous free energies of solvation based on pairwise descreening of solute atomic charges from a dielectric medium. *J. Phys. Chem*. 100:19824–19839.
52. Bondi, A. 1964. Van der Waals volumes and radii. *J. Phys. Chem*. 64:441–451.
53. Popenda, M., E. Biala, J. Milecki, and R. W. Adamiak. 1997. Solution structure of RNA duplexes containing alternating CG base pairs: NMR study of r(CGCGCG)2 and 2′-O-Me(CGCGCG)2 under low salt conditions. *Nucleic Acids Res*. 25:4589–4598.

54. Smith, J. S., and E. P. Nikonowicz. 1998. NMR structure and dynamics of an RNA motif common to the spliceosome branch-point helix and the RNA-binding site for phage GA coat protein. *Biochemistry.* 37:13486–13498.

55. Rosen, M. A., D. Live, and D. J. Patel. 1992. Comparative NMR study of A-bulge loops in DNA duplexes intrahelical stacking of A, A-A and A-A-A bulge loops. *Biochemistry.* 31:4004–4014.

56. Zacharias, M., and H. Sklenar. 1999. Conformational analysis of single-base bulges in A-form DNA and RNA using a hierarchical approach and energetic evaluation with a continuum solvent model. *J. Mol. Biol.* 289:261–275.

57. Tereshko, V., S. T. Wallace, N. Usman, F. E. Wincott, and M. Egli. 2001. X-ray crystallographic observation of ''in-line'' and ''adjacent'' conformations in a bulged self-cleaving RNA/DNA hybrid. *RNA.* 7:405–420.

58. Reiter, N. J., H. Blad, F. Abildgaard, and S. E. Butcher. 2004. Dynamics in the U6 RNA intramolecular stem-loop: a base flipping conformational change. *Biochemistry.* 43:13739–13747.

59. Schmitz, M., and I. Tinoco. 2000. Solution structure and metal-ion binding of the P4 element from bacterial RNase P RNA. *RNA.* 6:1212–1225.

60. Hart, K., B. Nyström, M. Öhman, and L. Nilsson. 2005. Molecular dynamics simulations and free energy calculation of base flipping in dsRNA. *RNA.* 11:609–618.

61. Schmitz, M. 2004. Change of RNAse P RNA function by a single base mutation correlates with perturbation of metal ion binding in P4 as determined by NMR spectroscopy. *Nucleic Acids Res.* 32:6358–6367.

62. Banavali, N. K., and A. D. MacKerell Jr. 2002. Free energy and structural pathways of base flipping in a DNA GCGC containing sequence. *J. Mol. Biol.* 319:141–160.

63. Grahn, E., T. Moss, C. Helgstrand, K. Fridborg, M. Sundaram, K. Tars, H. Lago, N. Stonehouse, D. Davis, P. Stockley, and L. Liljas. 2001. Structural basis of pyrimidine specificity in the MS2 RNA hairpin-coat-protein complex. *RNA.* 7:1616–1627.